DOI 10.1007/s11041-023-00877-3
Metal Science and Heat Treatment, Vol. 64, Nos. 11 – 12, March, 2023 (Russian Original Nos. 11 – 12, November – December, 2022)

ALUMINUM AND ALUMINUM ALLOYS

UDC 669.112:539.4

EFFECT OF TWO-STAGE SURFACE MODIFICATION ON THE STRUCTURE OF Al – 11% Si AND Al – 20% Si SILUMINS

Yu. A. Shlyarova,[1] D. V. Zagulyaev,[1] V. E. Gromov,[1] Yu. F. Ivanov,[2] V. V. Shlyarov,[1] and A. N. Prudnikov[1]

Translated from *Metallovedenie i Termicheskaya Obrabotka Metallov*, No. 12, pp. 34 – 42, December, 2022.

Original article submitted July 7, 2022.

Al – 11% Si hypoeutectic alloy and Al – 20% Si hypereutectic alloy are studied after two-stage modification of the surface, which combines electroerosion alloying and subsequent irradiation with a pulsed electron beam. The structure of the surface layer is determined after two variants of two-stage treatment. The two-stage treatment of alloy Al – 11% Si yields a multi-element multiphase layer with a thickness of about 80 μm and a submicro-nanocrystalline structure. The surface of alloy Al – 20% Si acquires two layers (a surface one and an intermediate one) differing in the structure from the silumin. The surface layer contains many phases and is up to 1 μm thick. The transition layer with a thickness of up to 40 μm is formed from rapid-crystallization cells produced by the high-rate cooling of the fused layer of alloy Al – 20% Si. The cells are separated by thin sublayers composed of chiefly silicon nanosize particles.

Key words: Al – 20% Si, Al – 11% Si, two-stage modifying, microstructure, surface layer, crystallization.

Modern machine building has to solve many important tasks such as creation of novel alloys or advancement of the characteristics of standard materials, development of new technologies, saving of power and resources by fabricating efficient materials for machines and production equipment, elevation of the reliability and endurance of parts, etc. The first to receive the load in operation of machines and mechanisms are the surface layers of the materials, which attract the highest attention of scientists [1 – 4]. The service life of machines and mechanisms is reduced during operation because their technical condition worsens because of the wear and damage of the parts. Millions of parts go to remelting every year due to the wear of their working surfaces, though there are ways for their reconditioning. The cost of the reconditioned parts is much lower than that of production of new ones, because reconditioning does not involve such costly operations as remelting (in utilization of the worn article), casting, forming, and mechanical treatment used to make a new part. In many cases, the wide commercial use of aluminum alloys, development and installation of resource-saving processes of their production, and creation of novel structural and precision materials with specified properties help to solve the problems mentioned [5 – 7].

It is known that 80% aluminum castings produced in the world are manufactured from Al – Si alloys (silumins). In contrast to pure aluminum, silumin has an elevated strength, hardness and corrosion resistance due to the presence of silicon, which is harder than aluminum [8]. This is the reason behind the development of hypereutectic silumins with silicon concentration exceeding about 12%. However, such a composition is characterized by the presence of inclusions of silicon, pores, cracks, etc., which lowers its operating properties [9 – 13].

Car pistons are often produced from eutectic and hypereutectic silumins with 12 – 25 wt.% Si. Modifying and microalloying improve the combination of the properties and

[1] Siberian State Industrial University, Novokuznetsk, Russia (e-mail: rubannikova96@mail.ru).
[2] Institute of High-Current Electronics of the Siberian Branch of the Russian Academy of Sciences, Tomsk, Russia.

TABLE 1. Chemical Compositions of Alloys Al – 11% Si and Al – 20% Si

Alloy	Content of elements, wt.%							
	Al	Si	Fe	Cu	Mn	Ni	Ti	Cr
Al – 11% Si	84.88	11.10	0.25	2.190	0.020	0.920	0.050	0.010
Al – 20% Si	78.52	20.28	1.14	0.072	0.015	0.006	0.006	0.001

TABLE 2. Modes of Electroexplosion Alloying and Subsequent Irradiation with Electron Beam of Al – 11% Si and Al – 20% Si Silumins

Mode	Electroexplosion alloying				Irradiation with pulsed electron beam			
	m_{Al}, mg	$m_{Y_2O_3}$, mg	U, kV	E_s, J/cm^2	W, keV	t_{pulse}, μsec	n	f, sec^{-1}
1	58.9	58.9	2.8	35	18	150	3	0.3
2	58.9	88.3	2.6	25				

Notations: m_{Al}) mass of aluminum foil; $m_{Y_2O_3}$) mass of Y_3O_3 powder; U) discharge voltage; E_s) energy density of electron beam; W) energy of accelerated electrons; t_{pulse}) duration of electron beam pulse; n) number of current pulses; f) pulse frequency.

raise the operating characteristics of such alloys [14 – 18]. Pistons serve under sliding friction, elevated temperatures and high loads, and these dangerous conditions require a high reliability and wear resistance from engine pistons. The rubbing surface of a piston should be protected from wear, and this is achieved by different methods. In the recent decades, researchers have studied the processes of interaction between intense pulsed energy beams (ion, electron and plasma ones) and materials and the application of such beams in industry.

Today, the most promising method of surface treatment of metals and alloys involves two stages, i.e., deposition of a coating and subsequent irradiation with an electron beam. These two stages combine a thermal impact on the surface of the material with alloying of the surface layer [19, 20]. This combined action on the structure and phase composition prolongs the life of parts of machines and mechanisms. Thus, surface treatment of hypereutectic silumins is a timely task of recent machine building.

The aim of the present work was to analyze the structural and phase transformations occurring in the surface layer of hypoeutectic (Al – 11% Si) and hypereutectic (Al – 20% Si) alloys subjected to a two-stage treatment.

METHODS OF STUDY

We studied hypoeutectic alloy Al – 11% Si and hypereutectic alloy Al – 20% Si. The content of the alloying elements in the silumins was determined by an x-ray spectrum analysis accurate to ± 10%. The results of this analysis are presented in Table 1.

The surface layer of the silumins was modified in two stages. The first stage consisted in electroexplosion alloying. The exploded conductors were aluminum foils; the powder sample was Y_2O_3 oxide. The alloying was conducted in a EVU 60/10 electric-discharge unit [21].

The sputtering was conducted in vacuum in the following way. A sample of Y_2O_3 powder was placed onto an aluminum foil clamped between two coaxial electrodes. A voltage was applied to it through a vacuum discharger, and the conductor exploded under the action of a high-density current. The products of the explosion in the form of a plasma component containing particles of Al and Y_2O_3 of different sizes rushed through the process chamber to the specimen, precipitated on it and fused the surface layers of the silumin. The surface of the treated article acquired a multiphase and multicomponent coating.

In the second sage, the surface was modified with a pulsed electron beam. The irradiation was conducted using a "SOLO" power unit designed and created in Tomsk at the Institute of High-Current Electronics of the Siberian Branch of the Russian Academy of Sciences [22] in an argon atmosphere at pressure of 0.02 Pa. The modes of the electroexplosion alloying and of the subsequent irradiation of the alloy are presented in Table 2. The optimum modes for electroexplosion alloying multiply raising the mechanical characteristics of the surface layer of silumins have been determined in [23] after analyzing six treatment variants.

The phase compositions and the structural parameters of the specimens were determined by an x-ray diffraction analysis (SRD-6000 diffractometer, copper K_α radiation). The phase compositions were analyzed using the PDF 4+ database and the POWDER CELL 2.4 software for full-profile analysis. The defective substructure, the morphology, and the local phase composition of the modified layers of the silumin

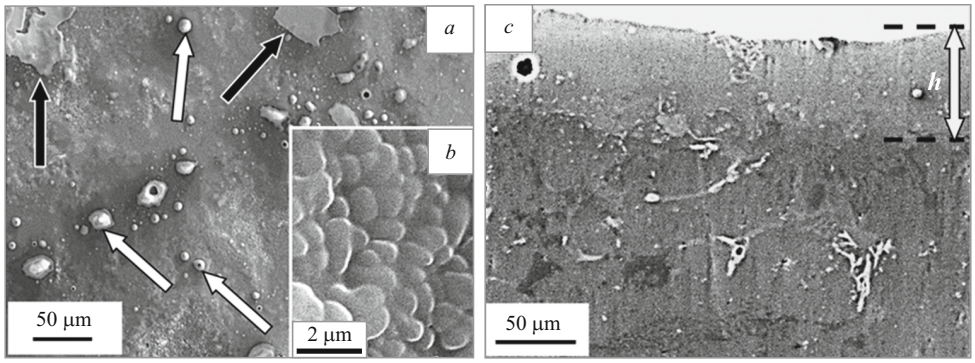

Fig. 1. Structure of the Al – 11% Si silumin after two-stage treatment *1*: *a*, *b*) irradiated surface (the light arrows point at micro drops; the dark arrows point at films); *c*) modified layer with thickness *h* (etched cross section).

specimens were studied by transmission electron microscopy (TEM) using a JEM 2100F microscope [24 – 26].

RESULTS AND DISCUSSION

A typical structure of the surface of the Al – 11% Si silumin after a two-stage treatment *1* is presented in Fig. 1. This treatment produces a surface containing micro craters, micro drops, and film inclusions (Fig. 1*a*). The formed surface layer has a submicrocrystalline structure; the sizes the crystallites do not exceed 1 μm (Fig. 1*b*). Analysis of the etched cross sections shows that the modified layer has a thickness $h = 70 – 80$ μm (Fig. 1*c*).

We analyzed the phase composition of the modified layer by TEM using dark-background imaging and deciphering of electron diffraction patterns [24 – 26, 30]. Figure 2*a* presents the structure of the modified layer of the Al – 11% Si silumin. The electron diffraction pattern from the region presented in Fig. 2*b* selected by the selector diaphragm contains a diffraction halo corresponding to an amorphous condition of the substance and reflections forming diffraction rings (Fig. 2*c*). Analyzing the electron diffraction patterns we detected reflection from silicon and from yttrium silicide SiY. The data of the x-ray spectrum analysis (Fig. 2*d*) allow is to think that the amorphous phase is a part of the surface (a film or a drop) enriched with yttrium. One of the phases with a nanocrystalline structure located on the interface of the drop and the bulk of the specimen is yttrium silicide SiY.

A typical structure of the surface of the specimen after treatment *2* is presented in Fig. 3. It can be seen that the two-stage treatment *2* produces a surface with a relief containing regions of different contrasts (Fig. 3*a*). The difference may indicate inhomogeneity of the elemental composition of the surface layer. It has a submicrocrystalline structure where the crystallites are no more than 1 μm in size (Fig. 3*b*).

The use of TEM allowed us to detect formation of a gradient submicro- and nanosize structure in the modified layer, a typical image of which is given in Fig. 4. It can be seen that the modified layer with a thickness of 70 μm has a structure of rapid cellular crystallization. The sizes of the cells vary from 0.5 to 1.2 μm. The cells are separated by layers of a second phase (Fig. 4*b*). The surface layer contains faceted inclusions (the dark particles in Fig. 4*a*) with a size ranging from 0.4 to 0.8 μm. The relative content of such inclusions decreases with the growth of the distance from the surface.

The morphology of the modified layer of the Al – 20% Si alloy was studied by TEM on foils prepared from plates cut form bulky specimens perpendicularly to the treatment surface. Figure 5*b* presents a typical structure of the layer formed after the two-stage treatment. Independently of the modification mode, this structure is a multilayer one and consists of a surface layer and intermediate layers (Fig. 5*a*).

The surface layer I consists of round-shape particles, the sizes of which range within about 10 – 20 nm (Fig. 5*b*). The thickness of the layer is about 1 μm. It can be assumed that these are particles of yttrium oxide modified as a result of the interaction with the fused surface layer of the substrate. The intermediate layer II has a structure of rapid cellular crystallization typical for a silumin treated with a pulsed electron beam in the mode of fusion of the surface layer [27, 28]. This layer contains globular inclusions composed of nanosize round particles (Fig. 5*c*). It can be assumed that these inclusions are conglomerates of particles of yttrium oxides. The thickness of the intermediate layer amounts to 30 – 40 μm and grows with the increase of the energy density of the electron beam.

Irradiation of the surface layer of the Al – 20% Si silumin with a pulsed electron beam with energy density 35 J/cm^2 after modification by the electroexplosion method causes formation of YSi_2 yttrium silicide. We have not detected this compound at a lower energy density of the electron beam.

The morphology, the sizes, and the distribution of phases in the surface layer of the Al – 20% Si silumin subjected to a two-stage treatment were studied by transmission electron

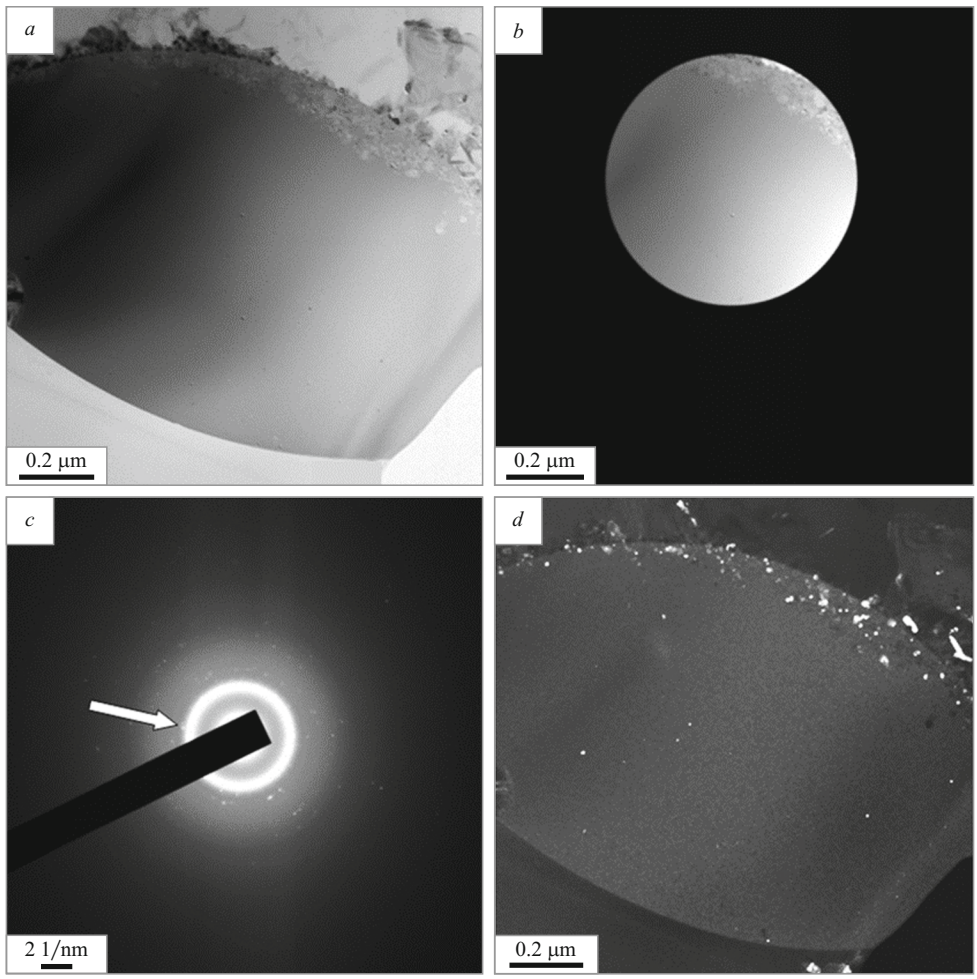

Fig. 2. Structure of the surface layer of the Al – 11% Si silumin after two-stage treatment *1*: *a*, *b*) against light background; *a*) general view; *b*) foil region chosen by the selector diaphragm; *c*) electron diffraction pattern from the region encircled in Fig. 2*b* ; *d*) dark background in reflection [211] of Si (marked with the arrow in Fig. 2*c*).

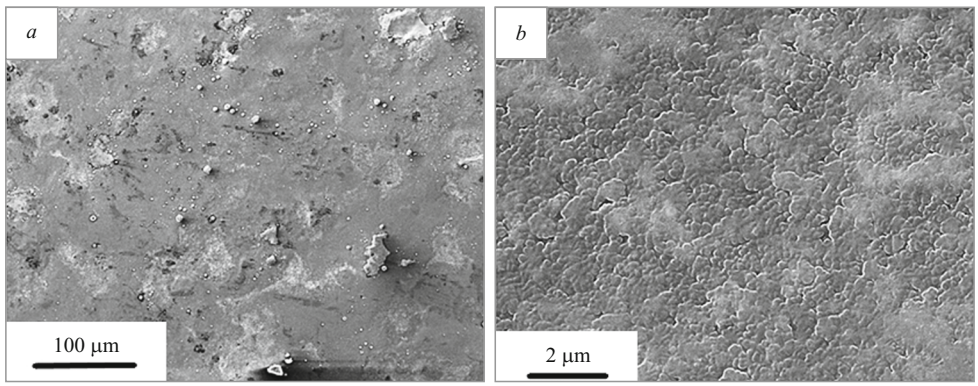

Fig. 3. Structure of the surface of the Al – 11% Si silumin modified by treatment *2*.

microscopy (light- and dark-background imaging and indexing of the electron diffraction patterns [29 – 31]). Figure 6*a* and *b* present the structure of the surface layer of Al – 20% Si and the microdiffraction from it. It can be seen in the dark-background images (Fig. 6*c* and *d*) that the surface layer is a nanostructured formation of round particles. The indexing of the electron diffraction pattern obtained from this layer (Fig. 6*b*) allowed us to detect the presence of YAl_3 of

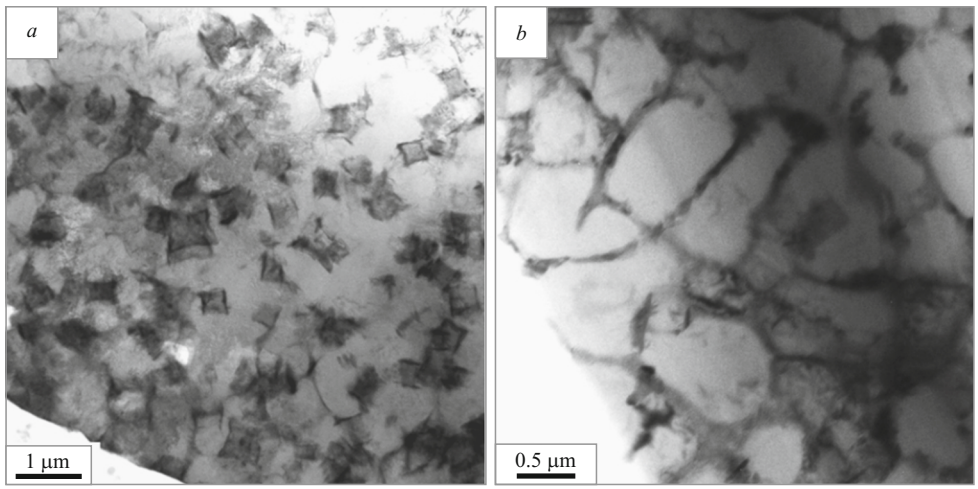

Fig. 4. Structure of the Al – 11% Si silumin after two-stage treatment *2*: *a*) surface layer; *b*) layer at a distance of 20 – 30 μm from the surface.

$Y_2Si_2O_7$ phases. It can be assumed that this surface layer has been formed as a result of interaction between the Y_2O_3 powder and the fused surface layer of the Al – 20% Si alloy, which has caused formation of phases from the elements present in the layer.

Figure 7 presents the structure of the transition layer. The layer is formed by cells of high-rate crystallization formed as a result of abrupt cooling of the fused layer. Analysis of the electron diffraction pattern gives us grounds to infer that the cells have a structure of an aluminum-base solid solution (Fig. 7*d*). The cells are separated by thin layers represented by nanosize particles. Indexing of the electron diffraction pattern shows that these particles consist of silicon (Fig. 7*c*).

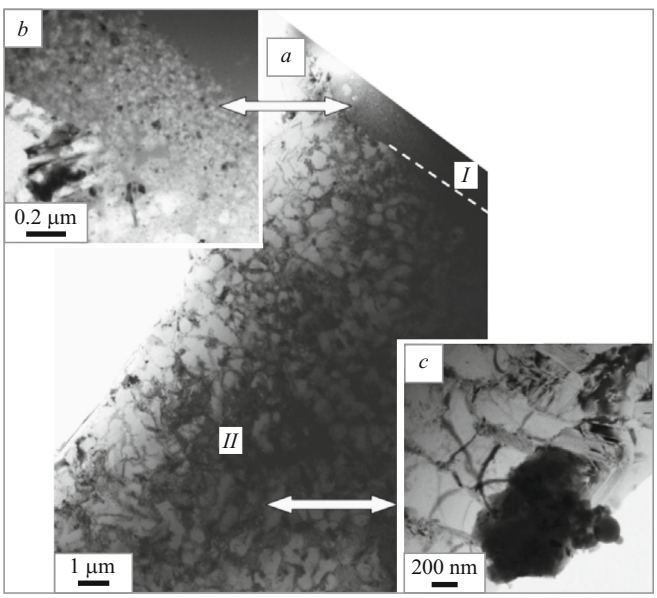

Fig. 5. Structure of the Al – 20% Si alloy after two-stage treatment: *a*) general view; *b*) surface layer; *c*) intermediate layer II.

The data of Fig. 7*c* allow us to state that the silicon layers located on the boundaries and at the junctions of the boundaries of the crystallization cells formed by the aluminum-base solid solution have a nanocrystalline structure with crystallites sizes of about 10 – 20 nm.

Figure 8 presents the structure of a foil region with a conglomerate of spherical particles. The analysis of the electron diffraction pattern obtained from this cluster allowed us to detect reflections belonging to the crystal lattice of phase $Y_2Si_2O_7$ (Fig. 8*b*). These data show that the conglomerates of particles of powder yttrium oxide that have got into the fused layer of alloy Al – 20% Si can be alloyed with its elements.

Thus the methods of TEM make it possible not only to study the morphology and the sizes of the second-phase particles but also to detect additional phases undetectable by the x-ray diffraction analysis due to their low content in the alloy.

CONCLUSIONS

We have studied alloy Al – 11% Si after a two-stage modifying involving electroexplosion alloying and subsequent irradiation with a high-intensity pulsed electron beam. Treatment *1* has yielded a multielement multiphase layer with a thickness of about 80 μm and a submicro-nanocrystalline structure. The modified surface contained stiff drops enriched with yttrium atoms and having an amorphous condition. Treatment *2* has caused a cardinal transformation of the structure of the surface layer with a thickness of about 70 μm, which consisted of dissolution of the inclusions of silicon and of the intermetallics typical for the cast state of the silumin and formation of a multielement submicro-nanosize structure.

We also studied the structure, the phase composition, and the condition of the defective substructure of specimens of alloy Al – 20% Si subjected to a two-stage treatment using

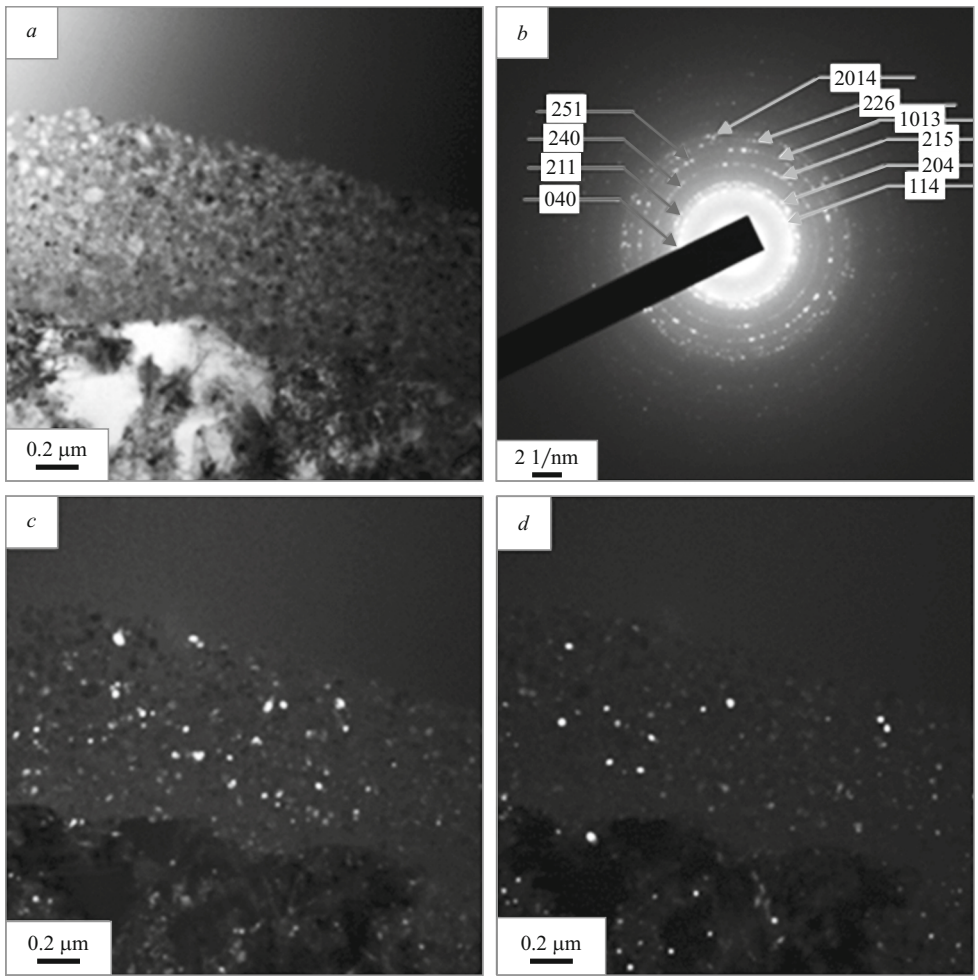

Fig. 6. Structure of the surface layer of the Al – 20% Si alloy after two-stage treatment: *a*) against light background; *b*) electron diffraction pattern (the yellow arrows point at diffraction rings from YAl_3; the red arrows point at diffraction rings from $Y_2Si_2O_7$); *c*, *d*) against dark background (from the rings in Fig. 6*b*); *c*) in reflections [204] of YAl_3, [300] of Y_5Si_3 and [211] of $Y_2Si_2O_7$; *d*) in reflections [1013] of YAl_3, [410] of Y_5Si_3 and [251] of $Y_2Si_2O_7$.

the methods of transmission electron diffraction microscopy and x-ray diffraction analysis. Independently of the mode of the modification, the surface of the silumin acquired two layers (a surface one and an intermediate one) which differed in the structure.

The surface layer with a thickness of about 1 μm was a multiphase material formed presumably as a result interaction between the Y_2O_3 powder and the fused layer of alloy Al – 20% Si. The transition layer with a thickness of about about 40 μm was represented by cells of rapid crystallization of the fused layer of the Al – 20% Si alloy. The cells were separated by thin interlayers of nanosize particles mostly represented by silicon. The volume of the transition layer also contained conglomerates of spherical particles formed from the powder yttrium oxide that had penetrated the fused layer and then was alloyed with the elements of the initial silumin. The intermediate layer formed as a result of the high-rate crystallization acquired solid solutions based on the crystal lattices of aluminum and silicon enriched with yttrium atoms.

The two-stage treatment involving electroexplosion alloying and subsequent irradiation by an electron beam may be recommended for modifying the surface of hypoeutectic and hypereutectic silumins.

The study has been financed by the Russian Scientific Foundation, Grant No. 19-79-10059, https://rscf.ru/project/19-79-10059/.

REFERENCES

1. A. Blutmager, M. Varga, U. Cihak-Bayr, et al., “Wear in hard metal check valves: In-situ surface modification through tribolayer formation in dry contact,” *Vacuum*, **192**, 110482 (2021).
2. H. Jiang, Z. Ren, Y. Yi, et al., “Effect of machining on performance enhancement of superficial layer of high-strength alloy steel,” *J. Mater. Res. Technol*., **14**, 1065 – 1079 (2021).

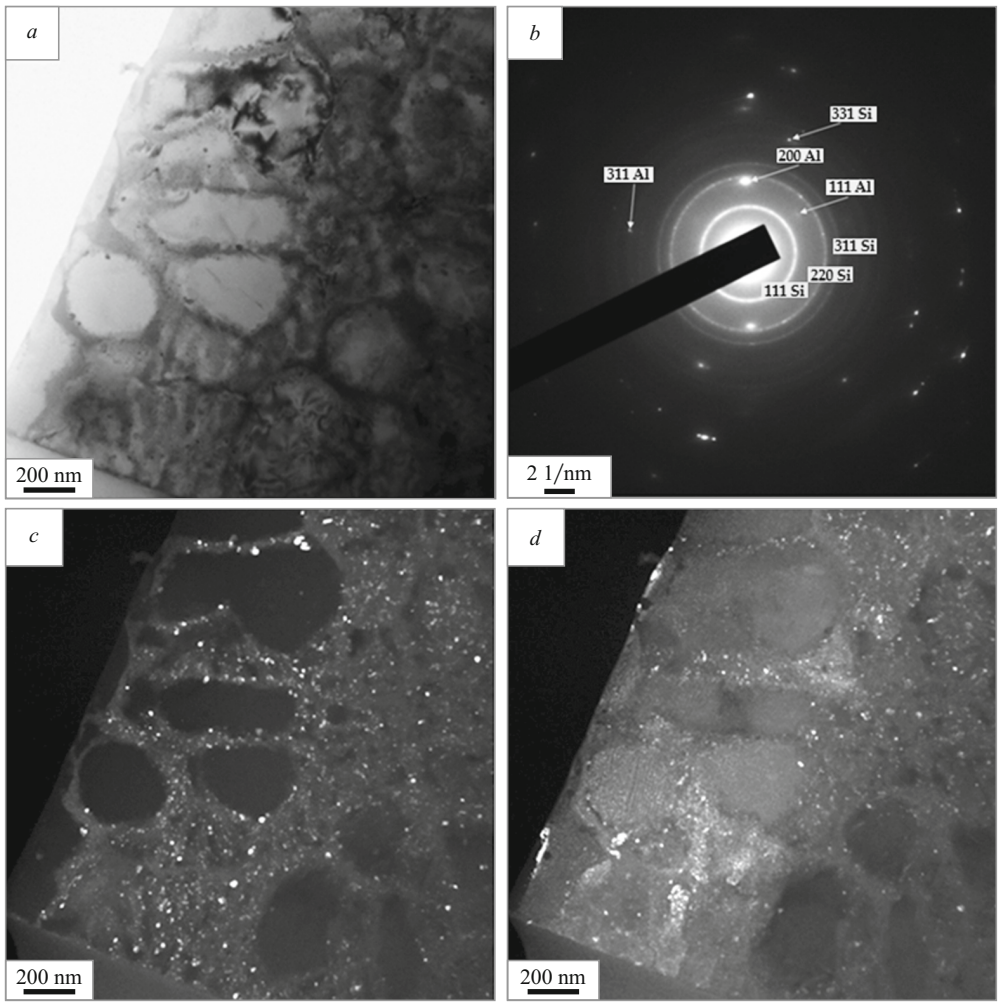

Fig. 7. Structure of the surface layer of the Al – 20% Si alloy after two-stage treatment: *a*) against light background; *b*) electron diffraction pattern; *c*, *d*) against dark background in reflections [220] of Si and [200] of Al, respectively.

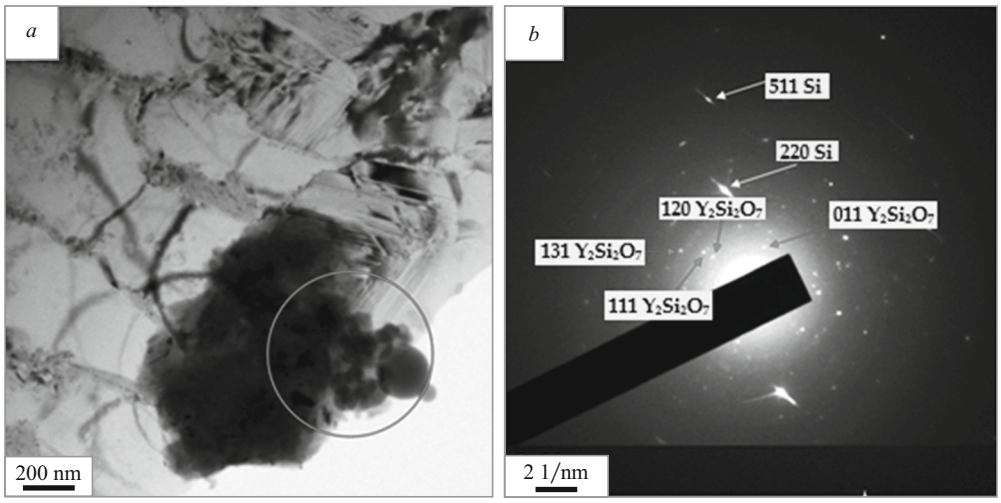

Fig. 8. Structure of the surface layer of the Al – 20% Si alloy after two-stage treatment: *a*, *c*) against light background; *b*) electron diffraction pattern from the region demarcated by the selector diaphragm in Fig. 8*a*.

3. Z. Liu, H. Zhang, Z. Yan, and P. Dong, "Enhanced fatigue performance of aluminum alloy through surface strengthening treatment," *Mater. Lett*., **306**, 130964 (2022).
4. J. Zhou, X. Han, H. Li, et al., "Investigation of layer-by-layer laser remelting to improve surface quality, microstructure, and mechanical properties of laser powder bed fused AlSi10Mg alloy," *Mater. Des*., **210**, 110092 (2021).
5. A. Kagramanian, P. Stankevich, D. Aulin, and A. Basov, "Efficiency improvement of locomotive-type diesel engine operation due to introduction of resource-saving technologies for cleaning diesel and diesel locomotive systems," *Proc. Comp. Sci.*, **149**, 264 – 273 (2019).
6. B. Denkena, M. A. Ditrich, Y. Liu, and M. Theuer, "Automatic regeneration of cemented carbide tools for a resource efficient tool production," *Proc. Manuf*., **21**, 259 – 265 (2018).
7. C. Fanghänel, A. Bautenstrauch, C. Symmank, et al., "Multidimensional analysis of process chains regarding the resource-efficient manufacturing of hybrid structures," *Proc. CIRP*, **26**, 595 – 600 (2015).
8. I. Palmear, D. StJohn, J. F. Nie, and M. Qian, *Metallurgy of the Light Metals*, Butterworth–Heinemann, Boston (2017), 544 p.
9. R. Li, L. Liu, L. Zhang, et al., "Effects of squeeze casting on microstructure and mechanical properties of hypereutectic Al – *x*Si alloys," J. Mater. Sci. Technol., **33**(4), 404 – 410 (2017).
10. J.-G. Jung, T.-Y. Ahn, Y.-H. Cho, et al., "Synergistic effect of ultrasonic melt treatment and fast cooling on the refinement of primary Si in a hypereutectic Al – Si alloy," *Acta Mater.*, **144**, 31 – 40 (2018).
11. Z. Lu, L. Zhang, J. Wang, et al., "Understanding of strengthening and toughening mechanisms for Sc-modified Al – Si – (Mg) series casting alloys designed by computational thermodynamics," *J. Alloys Compd*., **805**, 415 – 425 (2019).
12. Z. Cai, C. Zhang, R. Wang, et al., "Effect of solidification rate on the coarsening behavior of precipitate in rapidly solidified Al – Si alloy," *Progr. Nat. Sci., Mater. Int.*, **26**(4), 391 – 397 (2016).
13. Y. Birol, "Microstructural evolution during annealing of a rapidly solidified Al – 12Si alloy," *J. Alloys Compd*., **439**, 1 – 2, 81 – 86 (2007).
14. O. F. Farag, "Comparison of the effect of plasma treatment and gamma ray irradiation on PS – Cu nanocomposite films surface," *Res. Phys*., **9**, 91 – 99 (2018).
15. D. Wei, X. Wang, R. Wang, and H. Cui, "Surface modification of 5CrMnMo steel with scanning electron beam process," *Vacuum*, **149**, 118 – 123 (2018).
16. D. V. Zaguliaev, Yu. F. Ivanov, A. A. Klopotov, et al., "Evolution of strength properties and defect sub-structure of the hypoeutectic A319.0 alloy irradiated by a pulsed electron beam and fractured under tensile stress," *Materialia*, **20**, 101223 (2021).
17. D. Zaguliaev, Yu. Ivanov, S. Konovalov, et al., "Effect of pulsed electron beam treatment on microstructure and functional properties of Al – 5.4Si – 1.3Cu alloy," *Nuclear Instr. Methods Phys. Res., Sec. B, Beam Interaction Mater. Atoms*, **488**, 23 – 29 (2021).
18. N. Kang and M. E. L. Mansori, "A new insight on induced-tribological behavior of hypereutectic Al – Si alloys manufactured by selective laser melting," *Trib. Int*., 105751 (2020).
19. D. Zaguliaev, V. Gromov, Yu. Rubannikova, et al., "Structure and phase states modification of Al – 11Si – 2Cu alloy processed by ion-plasma jet and pulsed electron beam," *Surf. Coat. Technol*., **383**, 125246 (2020).
20. Yu. Ivanov, V. Gromov, D. Zaguliaev, A. Glezer, et al., "Modification of surface layer of hypoeutectic silumin by electroexplosion alloying followed by electron beam processing," *Mater. Lett*., **253**, 55 – 58 (2019).
21. Yu. Ivanov, E. A. Budovskikh, Y. D. Zhmakin, and V. E. Gromov, "Surface modification by the EVU 60/10 electroexplosive system," *Steel in Transl*., **41**(6), 464 – 468 (2011).
22. N. N. Koval and Yu. F. Ivanov, *Evolution of the Structure of the Surface Layer of Steel Subjected to Electron-Ion-Plasma Treatments* [in Russian], Izd. NTL, Tomsk (2016), 304 p.
23. V. E. Gromov, D. V. Zagulyaev, Yu. F. Ivanov, et al., *Structure and Hardening of Silumin Modified by Electron-Ion Plasma* [in Russian], Izd. Tsentr SinGIU, Novokuznetsk (2020), 285 p.
24. F. R. Egerton, *Physical Principles of Electron Microscopy*, Springer Int. Publ., Basel (2016), 196 p.
25. C. S. S. R. Kumar, *Transmission Electron Microscopy. Characterization of Nanomaterials*, Springer, New York (2014), 717 p.
26. C. B. Carter and D. B. Williams, *Transmission Electron Microscopy*, Springer Int. Publ., Berlin (2016), 518 p.
27. D. Zaguliaev, Yu. Ivanov, S. Konovalov, et al., "Effect of electron-plasma treatment on the microstructure of Al – 11 wt% Si alloy," *Mater. Res*., **23**(2), e20200057 (2020).
28. D. Zaguliav, S. Konovalov, Y. Ivanov, et al., "Microstructure and microhardness of piston alloy Al – 10Si – 2Cu irradiated by pulsed electron beam," *Arch. Foundry Eng*., **20**(3), 92 – 98 (2020).
29. O. A. Bannykh, P. B. Budberg, S. P. Alisova, et al., *Phase Diagrams of Iron-Based Binary and Multicomponent Systems* [in Russian], Metallurgiya, Moscow (1986), 440 p.
30. L. M. Utevskii, *Diffraction Electron Microscopy in Metals Science* [in Russian], Metallurgiya, Moscow (1973), 533 p.
31. G. Tomas and M. J. Goringe, *Transmission Electron Microscopy of Materials* [Russian translation], Nauka, Moscow (1983), 320 p.